Published OnlineFirst March 26, 2015; DOI: 10.1158/1940-6207.CAPR-15-0025-T

Research Article

Cancer Prevention Research

Ink4a/Arf-Dependent Loss of Parietal Cells Induced by Oxidative Stress Promotes CD44-Dependent Gastric Tumorigenesis

Ryo Seishima[1,2], Takeyuki Wada[2], Kenji Tsuchihashi[1], Shogo Okazaki[1], Momoko Yoshikawa[1], Hiroko Oshima[3], Masanobu Oshima[3], Toshiro Sato[4], Hirotoshi Hasegawa[2], Yuko Kitagawa[2], James R. Goldenring[5], Hideyuki Saya[1], and Osamu Nagano[1]

Abstract

Loss of parietal cells initiates the development of spasmolytic polypeptide–expressing metaplasia (SPEM), a precancerous lesion in stomach. CD44 variant (CD44v) that enhances the ability to defend against reactive oxygen species (ROS) in epithelial cells is expressed *de novo* in SPEM of *K19-Wnt1/C2mE* mice, a transgenic model of gastric tumorigenesis, and is required for the efficient development of SPEM and gastric tumor in these animals. The role of ROS and its downstream signaling in CD44-dependent gastric tumorigenesis has remained unknown, however. With the use of the *K19-Wnt1/C2mE* mouse, we now show that parietal cells in the inflamed stomach are highly sensitive to oxidative stress and manifest activation of $p38^{MAPK}$ signaling by ROS. Oral treatment with the antioxidant ascorbic acid or genetic ablation of the *Ink4a/Arf* locus, a major downstream target of ROS-$p38^{MAPK}$ signaling, inhibited parietal cell loss and the subsequent gastric tumorigenesis. Our results indicate that signaling activated by oxidative stress in parietal cells plays a key role in CD44-dependent gastric tumorigenesis. *Cancer Prev Res; 8(6); 492–501. ©2015 AACR.*

Introduction

Chronic inflammation induces histopathologic progression of the stomach epithelium leading to the development of metaplasia followed by gastric adenocarcinoma (1, 2). Oxyntic glands, the predominant type of gastric gland, comprise several types of fully differentiated epithelial cells, including acid-secreting parietal cells and pepsinogen-secreting chief cells. Inflammation of the gastric epithelium results in a gradual loss of parietal cells and their replacement with proliferative metaplastic cells derived from transdifferentiated chief cells (3, 4), suggesting that chronic inflammation disrupts homeostasis of the gastric epithelium by altering the viability or differentiation status of these differentiated cells. Spasmolytic polypeptide–expressing metaplasia (SPEM) is triggered by the parietal cell loss, and is recognized as a precancerous lesion (5, 6). Parietal cells, thus, play a key role in the homeostasis of gastric glands, with the loss of these cells being considered an early and critical event in the histopathologic progression of the stomach epithelium and eventual development of gastric cancer. The molecular mechanism underlying parietal cell loss has remained unclear, however.

Chronic inflammation followed by carcinogenesis is associated with the production of reactive oxygen species (ROS; refs. 7, 8). ROS function as activators of MAPK signaling, including the Ras–Raf–MEK1/2–ERK1/2 and $p38^{MAPK}$ signaling pathways, and they play opposing roles in tumor promotion and suppression (9, 10). In general, ROS-mediated activation of Ras–Raf–MEK1/2–ERK1/2 signaling is associated with carcinogenesis as a result of its promotion of cell survival and proliferation, whereas ROS-mediated activation of $p38^{MAPK}$ signaling inhibits cell proliferation and induces cell senescence through induction of the tumor-suppressor proteins $p16^{INK4a}$ and $p19^{ARF}$ (11). The functional relevance of ROS-mediated signaling in the development of metaplasia and gastric cancer has not been elucidated, however.

CD44 exists in numerous isoforms that are generated through alternative splicing of CD44 precursor mRNA (12–14). CD44 variant (CD44v) isoforms, which contain additional insertions in the membrane-proximal extracellular region, are highly abundant in epithelial-type carcinomas (15). We previously showed that interaction of CD44v with xCT (SLC7A11), a subunit of the cystine/glutamate antiporter system xc(−), stabilizes the latter protein, and thereby promotes glutathione synthesis and potentiates the ability of cancer cells to defend themselves against ROS (16). In gastric carcinogenesis, *de novo* expression of CD44v is associated with the development of SPEM (17) and gastric tumors (18), and CD44v was recently identified as a cell surface marker of gastric cancer stem cells (19). Consistent with these observations, we recently showed that potentiation of ROS defense by the CD44v-xCT system

[1]Division of Gene Regulation, Institute for Advanced Medical Research, School of Medicine, Keio University, Shinjuku-ku, Tokyo, Japan. [2]Department of Surgery, School of Medicine, Keio University, Shinjuku-ku, Tokyo, Japan. [3]Division of Genetics, Cancer Research Institute, Kanazawa University, Kanazawa, Japan. [4]Division of Gastroenterology and Hepatology, Department of Internal Medicine, School of Medicine, Keio University, Shinjuku-ku, Tokyo, Japan. [5]Nashville VA Medical Center and the Epithelial Biology Center, Vanderbilt University School of Medicine, Nashville, Tennessee.

Note: Supplementary data for this article are available at Cancer Prevention Research Online (http://cancerprevres.aacrjournals.org/).

Corresponding Author: Osamu Nagano, Keio University School of Medicine, 35 Shinano-machi, Shinjuku-ku, Tokyo 160-8582, Japan. Phone: 81-3-5363-3981; Fax: 81-3-5363-3982; E-mail: osmna@sb3.so-net.ne.jp

doi: 10.1158/1940-6207.CAPR-15-0025-T

Published OnlineFirst March 26, 2015; DOI: 10.1158/1940-6207.CAPR-15-0025-T

plays a key role not only in tumor cells, but also in the expansion of SPEM cells in the *K19-Wnt1/C2mE* mouse, a transgenic model of gastric cancer induced by activation of Wnt and prostaglandin E_2 (PGE_2) signaling pathways (17). The populations of CD44v-expressing metaplastic cells and tumor cells in which ROS defense is bolstered by the CD44v-xCT system might, thus, be able to expand preferentially in inflamed gastric epithelium exposed to high levels of ROS. However, the role of ROS and its downstream signaling in CD44-dependent gastric tumorigenesis has remained unknown.

Materials and Methods

Animals

K19-Wnt1/C2mE transgenic mice, *Ink4a/Arf*$^{-/-}$ mice and *CD44*$^{-/-}$ *K19-Wnt1/C2mE* mice were described as previously (16, 20, 21). *K19-Wnt1/C2mE* transgenic mice were crossed with *Ink4a/Arf*$^{-/-}$ mice to generate *Ink4a/Arf*$^{-/-}$ *K19-Wnt1/C2mE* mice. All animal experiments were performed according to protocols approved by the Ethics Committee of Keio University. All efforts were made to minimize the suffering of animals used in this study.

Tamoxifen injection

Tamoxifen (Sigma-Aldrich) was injected i.p. at a daily dose of 250 mg/kg in WT or *Ink4a/Arf*$^{-/-}$ mice for 3 days, and tissue was dissected for analysis at 3 days after the last injection. *K19-Wnt1/C2mE* mice at 20 weeks of age were injected i.p. with tamoxifen (250 mg/kg) once a week for 5 weeks. Tamoxifen was dissolved in a vehicle consisting of 10% ethanol and 90% sunflower seed oil (Sigma-Aldrich), and control mice were injected with vehicle alone.

Immunohistochemistry

Immunohistochemistry was performed as previously reported (16, 17). TFF2 was detected with rabbit monoclonal antibodies (diluted 1:100; Proteintech).The TFF2-positive area in five randomly selected microscopic fields (magnification, ×40) per section was measured with the use of analysis software (BZ-9000; Keyence), and the mean percentage positive area was calculated. Parietal cells were detected with mouse monoclonal antibodies to the β subunit of H^+,K^+-ATPase (MBL). The mean percentage of H^+,K^+-ATPase–positive cells per gland in five microscopic fields per mouse was calculated. CD44v8-10 was detected with a rat monoclonal antibody (diluted 1:100; ref. 16), and the proportion of positive cells was determined with the use of a TissueFAXS cell analysis system (Novel Science).

Immunoblot analysis

Immunoblot analysis was performed as described previously (16, 17).

Gastric unit isolation and gastric organoid culture

Gastric gland units were isolated as previously described (22). Other experimental procedures are described in Supplementary Materials and Methods.

Statistical analysis

Data are presented as means ± SD and were analyzed with the unpaired Student *t* test as performed with the use of Microsoft Excel 2007. A P value of <0.05 was considered statistically significant.

Results

Depletion of ROS suppresses gastric tumorigenesis in *K19-Wnt1/C2mE* mice

To explore the relevance of ROS in gastric carcinogenesis, we orally administered ascorbic acid, a potent water-soluble antioxidant, to *K19-Wnt1/C2mE* mice from 12 to 30 weeks of age. Tumors were markedly smaller in the ascorbic acid–treated *K19-Wnt1/C2mE* mice than in untreated control animals at 30 weeks of age (Fig. 1A and B), suggesting that gastric tumorigenesis is promoted by ROS in these mice.

Given that CD44v promotes ROS defense in tumor cells in this model (17), expansion of the CD44v-expressing tumor cells might be the result of selection by ROS in the tumor microenvironment. We therefore investigated CD44v expression in gastric tumors of *K19-Wnt1/C2mE* mice treated with ascorbic acid. The relative area occupied by CD44v-expressing cells in tumors was markedly reduced by ascorbic acid treatment (Fig. 1C), suggesting that CD44v-expressing tumor cells expand preferentially compared with CD44v-negative cells in the presence of ROS. The expression of CD44v in epithelial cells of the normal foregut was not diminished by ascorbic acid treatment, however, suggesting that ROS depletion suppresses the selective expansion of ROS-resistant CD44v-expressing tumor cells without affecting normal epithelial cells in *K19-Wnt1/C2mE* mice.

Given that SPEM is a premalignant lesion (4), we next investigated whether CD44v-expressing SPEM cells might be the cells of origin for CD44v-expressing tumor cells. We thus examined whether ROS depletion by ascorbic acid treatment was able to reduce not only the number of CD44v-expressing tumor cells, but also that of CD44v-expressing SPEM cells in *K19-Wnt1/C2mE* mice. Formation of trefoil factor 2 (TFF2)–expressing SPEM was significantly suppressed in ascorbic acid–treated mice (Fig. 1D and E), indicating that ROS promotes CD44v-expressing SPEM formation as well as tumor formation.

Given that the parietal cell loss is a key event in SPEM development, we next examined the expression of the β subunit of H^+,K^+-ATPase, a marker of parietal cells. Immunohistochemical analysis revealed that the loss of parietal cells was significantly attenuated in ascorbic acid–treated mice (Fig. 1D and F), implicating ROS in the parietal cell loss apparent in untreated *K19-Wnt1/C2mE* mice. Analysis of the expression of CD44v in epithelium adjacent to tumors of *K19-Wnt1/C2mE* mice revealed that the emergence of CD44v-expressing SPEM cells was markedly suppressed by ascorbic acid treatment (Fig. 1D). Thus, ROS play a key role in parietal cell loss leading to the development of SPEM comprising CD44v-expressing SPEM cells.

$p38^{MAPK}$ is activated specifically in gastric parietal cells of *K19-Wnt1/C2mE* mice

To examine whether oxidative stress–induced signaling is operative in parietal cells of *K19-Wnt1/C2mE* mice, we investigated the activation status of $p38^{MAPK}$, a major target of ROS. The phosphorylated (activated) form of $p38^{MAPK}$ (phospho-$p38^{MAPK}$) was found to be abundant in parietal cells of *K19-Wnt1/C2mE* mice (Fig. 2A), suggesting that ROS accumulate in these cells. To address this possibility further, we measured ROS

Published OnlineFirst March 26, 2015; DOI: 10.1158/1940-6207.CAPR-15-0025-T

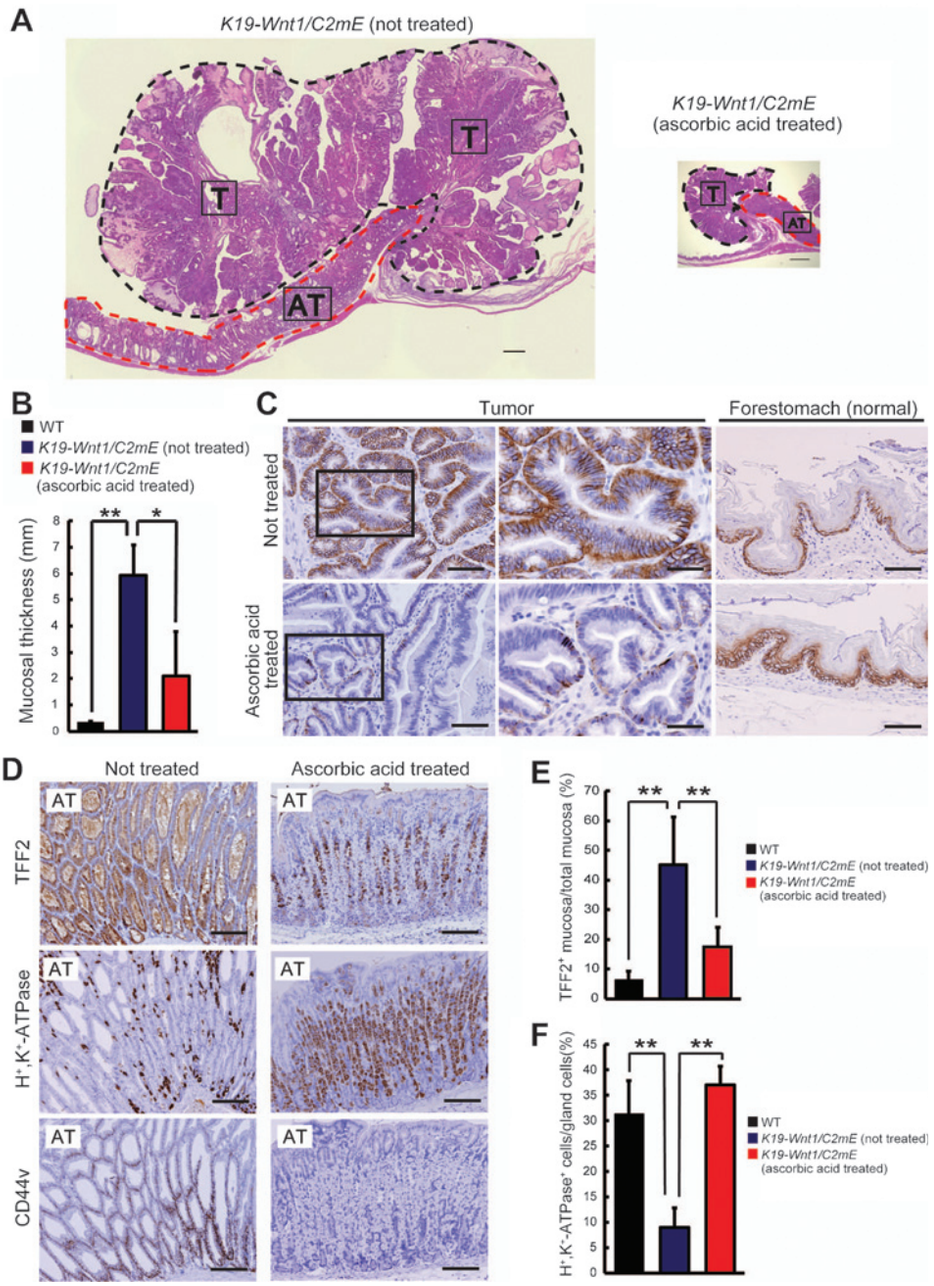

Figure 1.
Effects of ascorbic acid on development of gastric tumors and SPEM. A, hematoxylin and eosin (H&E) staining of gastric tumors of *K19-Wnt1/C2mE* mice treated (or not) with ascorbic acid from 12 to 30 weeks of age. The black and red dashed lines indicate the tumor boundary and adjacent regions, respectively; T, tumor; AT, region adjacent to tumor; scale bars, 500 μm. B, mucosal thickness, which reflects the size of the tumor, in *K19-Wnt1/C2mE* mice treated (or not) with ascorbic acid from 12 to 30 weeks of age ($n = 3$ and 5, respectively) relative to that in wild-type (WT) mice ($n = 5$). Data, means ± SD for the indicated numbers of mice; *, $P < 0.05$; **, $P < 0.01$ (Student *t* test). C, immunohistochemical staining for CD44v in gastric tumors of *K19-Wnt1/C2mE* mice treated (or not) with ascorbic acid from 12 to 30 weeks of age. The boxed regions in the left are shown at higher magnification in the middle. Staining for CD44v in the foregut is also shown in the right as a positive control; scale bars, 200 μm (left and right) or 100 μm (middle). D, immunohistochemical analysis of TFF2, the β subunit of H^+,K^+-ATPase and CD44v in regions adjacent to gastric tumors of *K19-Wnt1/C2mE* mice treated (or not) with ascorbic acid from 12 to 30 weeks of age; scale bars, 200 μm. E, mean area of $TFF2^+$ epithelium determined from sections similar to those in D. Data, means ± SD for 3 or 5 *K19-Wnt1/C2mE* mice treated or not treated with ascorbic acid, respectively, as well as for the normal gastric epithelium of five WT mice; **, $P < 0.01$ (Student *t* test). F, the mean percentage of H^+,K^+-ATPase–positive cells per gland in five microscopic fields per mouse was calculated in tumor-adjacent regions of sections similar to those in D. Data, means ± SD for the numbers of animals indicated in E; **, $P < 0.01$ (Student *t* test).

levels in parietal cells and nonparietal gastric cells isolated from wild-type (WT) and *K19-Wnt1/C2mE* mice. Flow cytometric analysis of cells stained with 2′,7′-dichlorofluorescein diacetate (DCFH-DA) revealed that DCFH-DA fluorescence intensity was much higher in parietal cells of *K19-Wnt1/C2mE* mice than in nonparietal cells of the same animals or in parietal cells or nonparietal cells of WT mice (Fig. 2B), suggesting that ROS activates $p38^{MAPK}$ signaling in parietal cells.

To examine further whether $p38^{MAPK}$ is activated selectively in parietal cells of the stomach epithelium in the presence of high ROS levels, we exposed WT mice to ionizing radiation at a dose of 10 Gy to induce ROS production. The abundance of phospho-$p38^{MAPK}$ was increased selectively in parietal cells of the irradiated mice (Fig. 2C), suggesting that parietal cells are highly sensitive to oxidative stress. We also examined the sensitivity of $p38^{MAPK}$ activity in parietal cells to ROS with the use of a gastric organ culture system (Fig. 2D). Exposure of normal gastric mucosa to the oxidative stressor hydrogen peroxide (H_2O_2) induced $p38^{MAPK}$ activation specifically in parietal cells, and this activation was attenuated in the additional presence of ascorbic acid or the specific $p38^{MAPK}$ inhibitor SB203580 (Fig. 2E). Together, these results indicated that parietal cells have a low capacity for ROS defense, and therefore might be a major target for ROS during gastric carcinogenesis.

Published OnlineFirst March 26, 2015; DOI: 10.1158/1940-6207.CAPR-15-0025-T

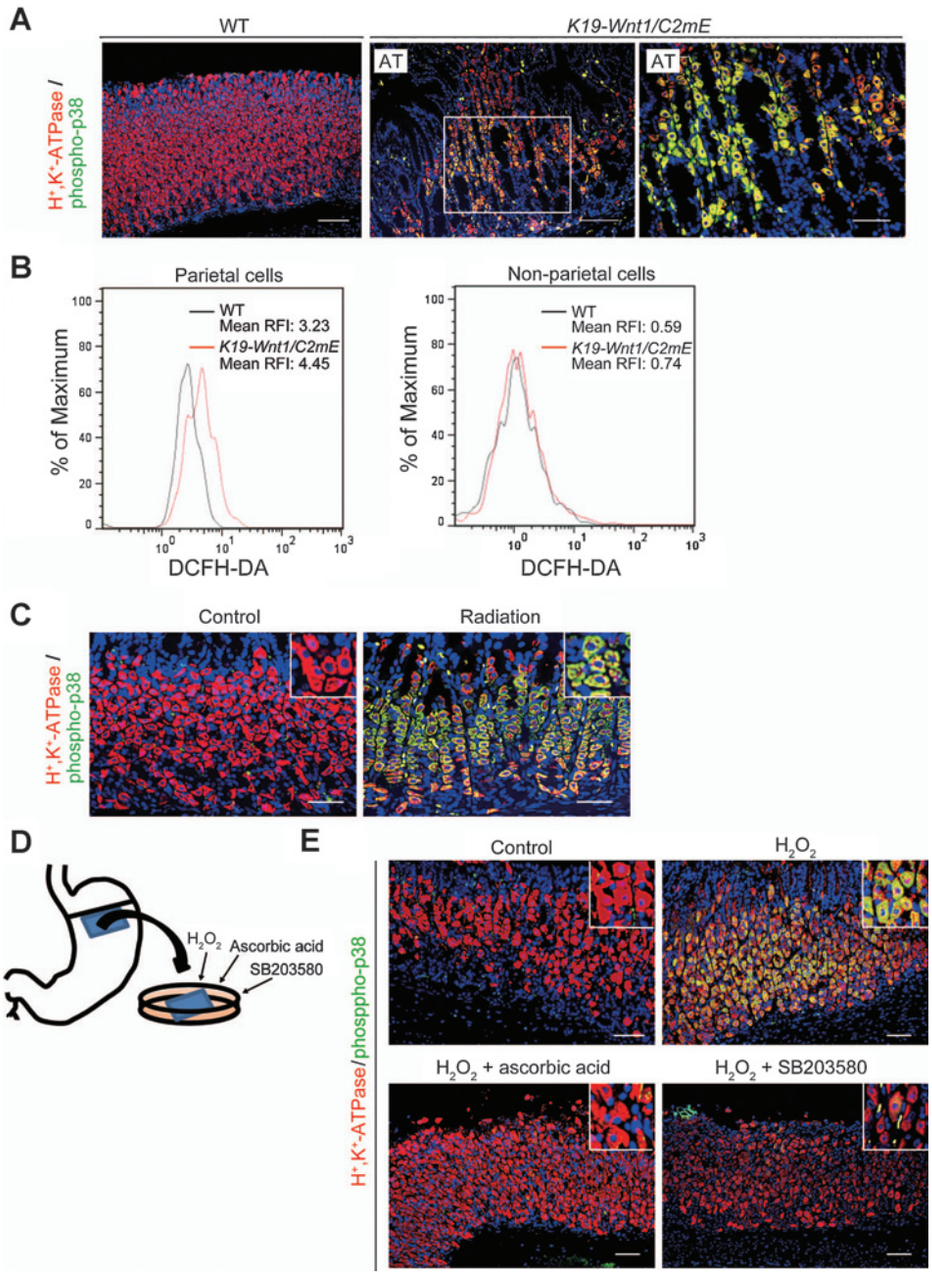

Figure 2.
ROS induce activation of $p38^{MAPK}$ specifically in parietal cells. A, immunohistofluorescence staining of H^+,K^+-ATPase (red) and phospho-$p38^{MAPK}$ (green) as well as staining of nuclei with 4′,6-diamidino-2-phenylindole (DAPI, blue) in the gastric epithelium of a WT mouse as well as in a gastric tumor–adjacent region (AT) of a *K19-Wnt1/C2mE* mouse at 30 weeks of age. The boxed region in the middle is shown at higher magnification in the right; scale bars, 200 μm (left and middle) or 100 μm (right). B, sorted parietal cells and nonparietal cells from SPEM lesions of *K19-Wnt1/C2mE* mice at 30 weeks of age and those from the glandular stomach of WT mice were stained with DCFH-DA and subjected to flow cytometric analysis; RFI, relative fluorescence intensity. C, immunohistofluorescence staining of H^+,K^+-ATPase and phospho-$p38^{MAPK}$ as well as staining of nuclei with DAPI in the gastric epithelium either of a WT mouse exposed to 10 Gy of ionizing radiation or of a nonirradiated control mouse. Insets show corresponding higher magnification images; scale bars, 100 μm. D, schematic representation of gastric organ culture. E, immunohistofluorescence staining of H^+,K^+-ATPase and phospho-$p38^{MAPK}$ as well as staining of nuclei with DAPI in stomach tissue of WT mice cultured for 6 hours in the absence or presence of 500 μmol/L H_2O_2, ascorbic acid (50 μg/mL) and 10 μmol/L SB203580 as indicated. Insets show corresponding higher magnification images; scale bars, 100 μm.

Parietal cell loss is triggered by ROS–$p38^{MAPK}$–$p16^{INK4a}$/$p19^{ARF}$ signaling

Given that activated $p38^{MAPK}$ has been shown to induce gene expression at the *Ink4a/Arf* locus, which encodes $p16^{INK4a}$ and $p19^{ARF}$, in cells exposed to oxidative stress (10), we next examined whether the expression of these proteins is increased in SPEM lesions of *K19-Wnt1/C2mE* mice. The abundance of $p16^{INK4a}$ and $p19^{ARF}$ as well as that of phospho-$p38^{MAPK}$ were markedly increased in SPEM of *K19-Wnt1/C2mE* mice compared with normal gastric mucosa of WT mice (Fig. 3A), suggesting that the $p38^{MAPK}$–$p16^{INK4a}$/$p19^{ARF}$ pathway is activated in SPEM.

To investigate the functional relevance of $p16^{INK4a}$ and $p19^{ARF}$ to parietal cell loss, we examined the effects of i.p. injection of tamoxifen, a potent inducer of parietal cell loss (23), in *Ink4a/Arf* knockout (*Ink4a/Arf*$^{-/-}$) mice. Immunohistochemical analysis revealed that the tamoxifen-induced parietal cell loss was markedly suppressed in *Ink4a/Arf*$^{-/-}$ mice compared with WT mice (Fig. 3B and C), suggesting that the *Ink4a/Arf* locus is essential for this effect of tamoxifen. The area of TFF2-positive mucosa was also substantially smaller in tamoxifen-treated *Ink4a/Arf*$^{-/-}$ mice than in tamoxifen-treated WT mice (Fig. 3B and D). Together, these results suggested that the *Ink4a/Arf* locus is required for the parietal cell loss, which plays a role in the development of SPEM in tamoxifen-treated mice.

Published OnlineFirst March 26, 2015; DOI: 10.1158/1940-6207.CAPR-15-0025-T

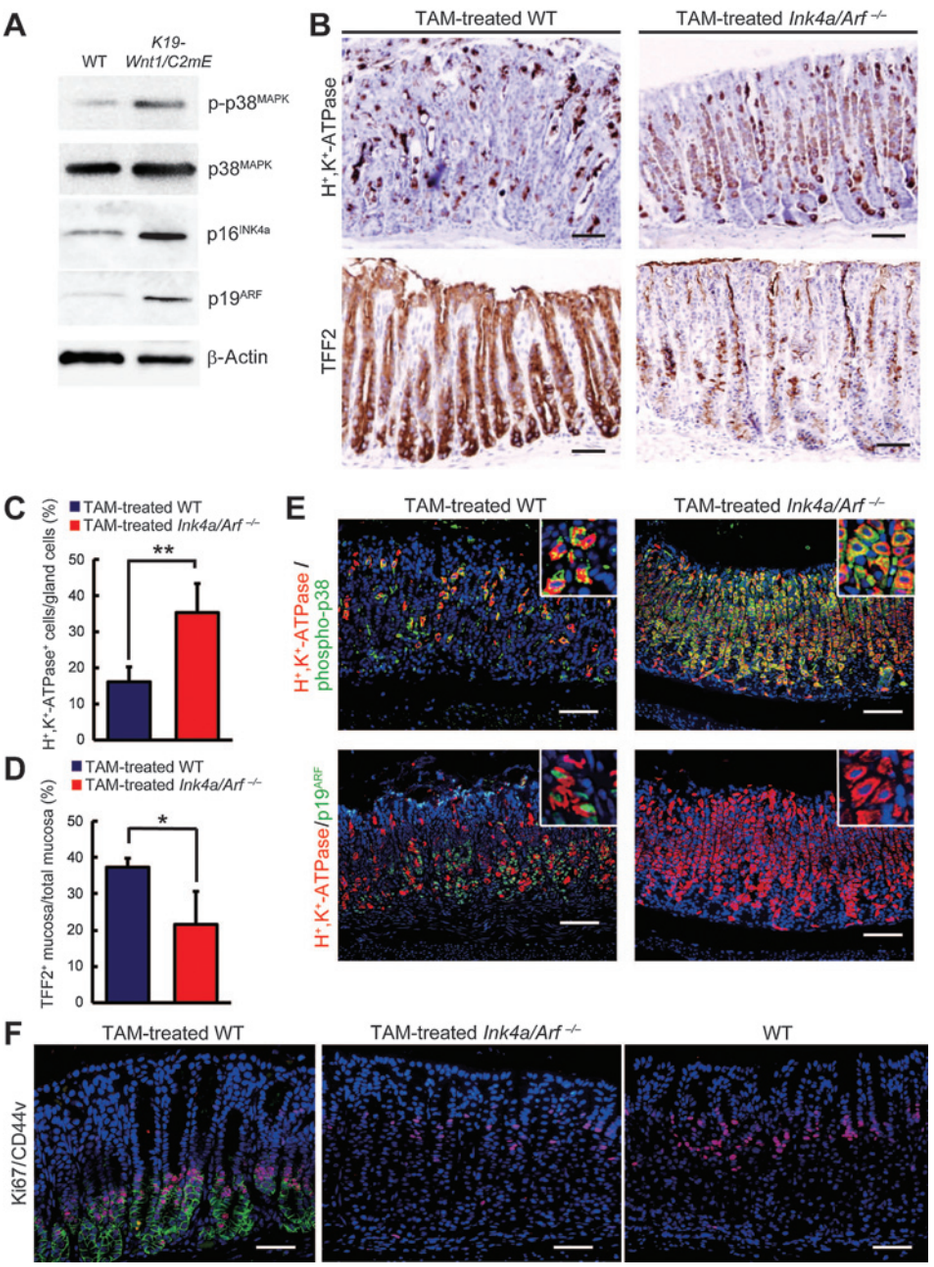

Figure 3.
The *Ink4a/Arf* locus is essential for parietal cell loss. A, immunoblot analysis of $p16^{INK4a}$, $p19^{ARF}$, and phosphorylated (p-) and total forms of $p38^{MAPK}$ in SPEM of 30-week-old *K19-Wnt1/C2mE* mice and in normal gastric mucosa of WT mice. β-Actin was analyzed as a loading control. B, immunohistochemical staining of H^+,K^+-ATPase and TFF2 in gastric mucosa of WT or *Ink4a/Arf*$^{-/-}$ mice at 3 days after daily i.p. injection with tamoxifen (TAM) for 3 days; scale bars, 100 μm. C, the mean percentage of H^+, K^+-ATPase–positive cells per gland in five microscopic fields per mouse was calculated in gastric mucosa from sections similar to those in B. Data, means ± SD for five tamoxifen-treated WT or *Ink4a/Arf*$^{-/-}$ mice; $^{**}P < 0.01$ (Student *t* test). D, mean area of $TFF2^+$ gastric epithelium determined from sections similar to those in B. Data, means ± SD for the numbers of animals indicated in C; *, $P < 0.05$ (Student *t* test). E, immunohistofluorescence staining of H^+,K^+-ATPase and either phospho-$p38^{MAPK}$ or $p19^{ARF}$ in gastric mucosa of tamoxifen-treated WT or *Ink4a/Arf*$^{-/-}$ mice. Nuclei were also stained with DAPI (blue). Insets show corresponding higher magnification images; scale bars, 100 μm. F, immunohistofluorescence staining of Ki67 and CD44v as well as staining of nuclei with DAPI in gastric mucosa of tamoxifen-treated WT or *Ink4a/Arf*$^{-/-}$ mice as well as of a nontreated WT mouse; scale bars, 100 μm.

We next investigated the abundance of phospho-$p38^{MAPK}$ and $p19^{ARF}$ in tamoxifen-treated mice. Immunofluorescence analysis revealed that phospho-$p38^{MAPK}$ and $p19^{ARF}$ were highly expressed in the few remaining parietal cells of tamoxifen-treated WT mice (Fig. 3E). The number of phospho-$p38^{MAPK}$–positive parietal cells in *Ink4a/Arf*$^{-/-}$ mice after tamoxifen treatment was much higher than that in WT mice (Fig. 3E), suggesting that activation of $p38^{MAPK}$ and downstream $p19^{ARF}$ expression contribute to tamoxifen-induced parietal cell loss.

To examine whether the parietal cell loss induced by tamoxifen results in the generation of CD44v-expressing metaplastic cells in the gastric epithelium, we performed immunofluorescence analysis of CD44v and the proliferation marker Ki67. Injection of tamoxifen effectively depleted parietal cells in WT mice (Supplementary Fig. S1). Proliferative CD44v-expressing cells were found to emerge from the base of gastric glands in tamoxifen-treated WT mice, whereas this phenomenon was greatly attenuated in tamoxifen-treated *Ink4a/Arf*$^{-/-}$ mice (Fig. 3F). These results suggested that the induction of *Ink4a/Arf* expression plays a key role in the parietal cell loss, and that such parietal cell loss triggers the generation of proliferative CD44v-expressing metaplastic cells.

SPEM contains stem-like cells capable of generating gastric glands

Given that CD44v is a gastric cancer stem cell marker (19) and plays a key role in SPEM development (16), we next

Published OnlineFirst March 26, 2015; DOI: 10.1158/1940-6207.CAPR-15-0025-T

examined whether SPEM induced by tamoxifen treatment contains stem-like cells that possess the ability to reconstitute a gastric gland. To assess the stem cell potential of gastric epithelial cells, we isolated a 5-mm square piece of glandular mucosa from the stomach of mice treated (or not) with tamoxifen for evaluation of the ability to form gastric organoids (Fig. 4A; ref. 24). The number of gastric organoids generated by the TFF2-expressing gastric mucosa resected from WT mice treated with tamoxifen (Fig. 4B) was markedly increased compared with that for the gastric mucosa of nontreated mice (Fig. 4C), suggesting that SPEM tissue contains a much higher number of stem-like cells than does normal stomach mucosa. We next investigated CD44v expression in the gastric organoids. Immunofluorescence analysis revealed that organoids derived from both tamoxifen-treated and untreated WT mice contained CD44v-expressing stem-like cells, although the number of such cells was greatly increased for organoids formed by SPEM compared with those formed by normal gastric mucosa (Fig. 4D). These results suggested that CD44v-expressing stem-like cells are generated by the mechanically damaged epithelial tissue derived from normal gastric mucosa, and that parietal cell loss further increases the number of such stem-like cells in tamoxifen-induced SPEM.

Given that tamoxifen-induced parietal cell loss and subsequent SPEM development were suppressed in the stomach of *Ink4a/Arf*$^{-/-}$ mice, we next examined the role of the *Ink4a/Arf* locus in tamoxifen-induced gastric organoid formation. The number of organoids formed by gastric mucosa from tamoxifen-treated mice was significantly reduced by genetic ablation of the *Ink4a/Arf* locus as well as that of *CD44* (Fig. 4E and F), suggesting that *Ink4a/Arf*–dependent parietal cell loss induces the expansion of CD44v-expressing stem-like cells.

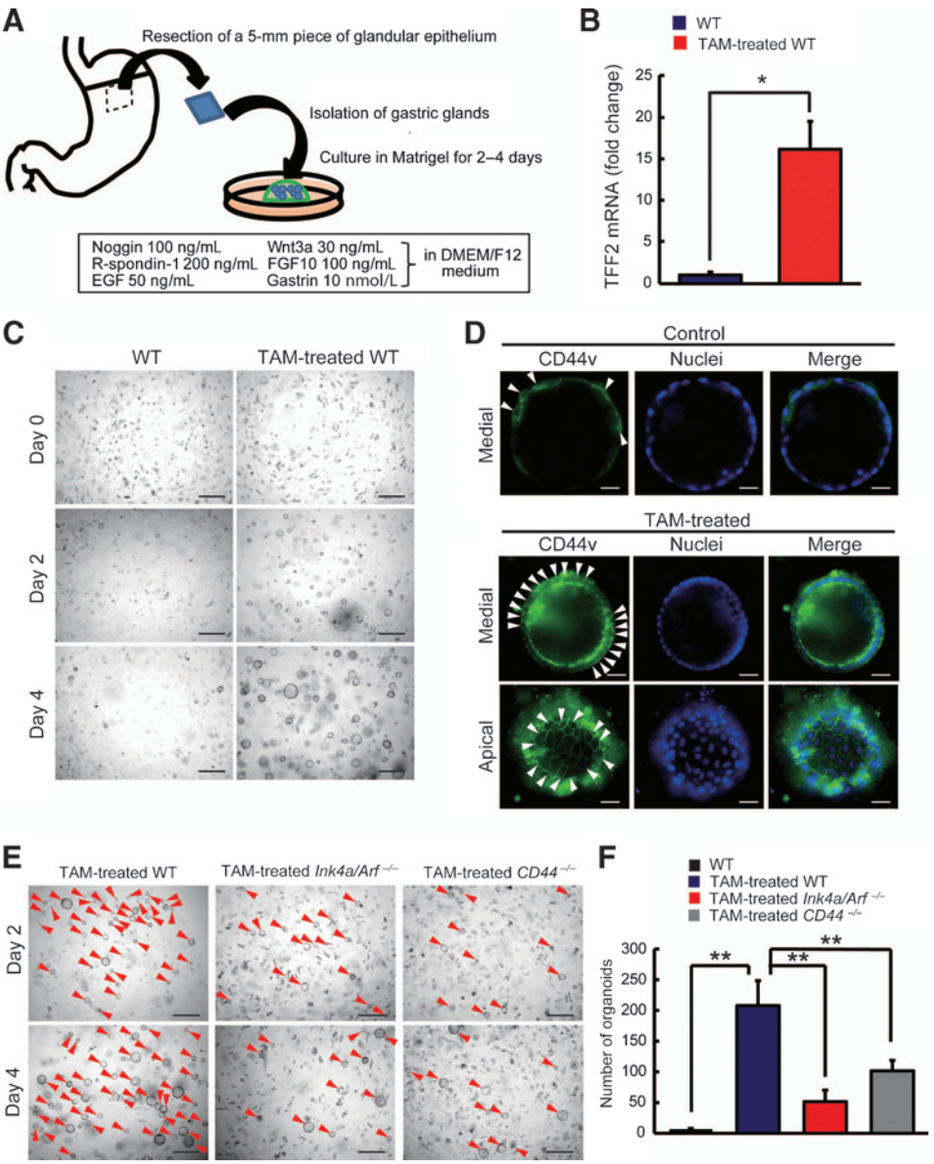

Figure 4.
SPEM induced by tamoxifen contains abundant stem-like cells. A, schematic representation of gastric gland isolation and organoid culture. B, quantitative RT-PCR analysis of TFF2 mRNA in glandular epithelium from tamoxifen-treated or untreated WT mice. Data were normalized by the amount of GAPDH mRNA and are means ± SD for 3 mice; *, $P < 0.05$ (Student *t* test). C, bright-field images of organoids derived from a single 5-mm square piece of gastric glandular epithelium from tamoxifen-treated or untreated WT mice. The representative images were acquired after culture for 0, 2, or 4 days; scale bars, 500 μm. D, immunohistofluorescence staining of CD44v (green) as well as staining of nuclei with DAPI (blue) in gastric organoids derived from tamoxifen-treated or control WT mice after culture for 4 days. The medial and apical sections of organoids are shown. Arrowheads show CD44v-positive cells; scale bars, 25 μm. E, bright-field images of organoids (arrowheads) derived from tamoxifen-treated WT or *Ink4a/Arf*$^{-/-}$ mice after culture for 2 or 4 days; scale bars, 500 μm. F, mean number of organoids derived from individual 5-mm square pieces of gastric glandular epithelium from tamoxifen-treated WT, *Ink4a/Arf*$^{-/-}$ and *CD44*$^{-/-}$ mice or from untreated WT mice. Data, means ± SD for 4 mice; **, $P < 0.01$ (Student *t* test).

Published OnlineFirst March 26, 2015; DOI: 10.1158/1940-6207.CAPR-15-0025-T

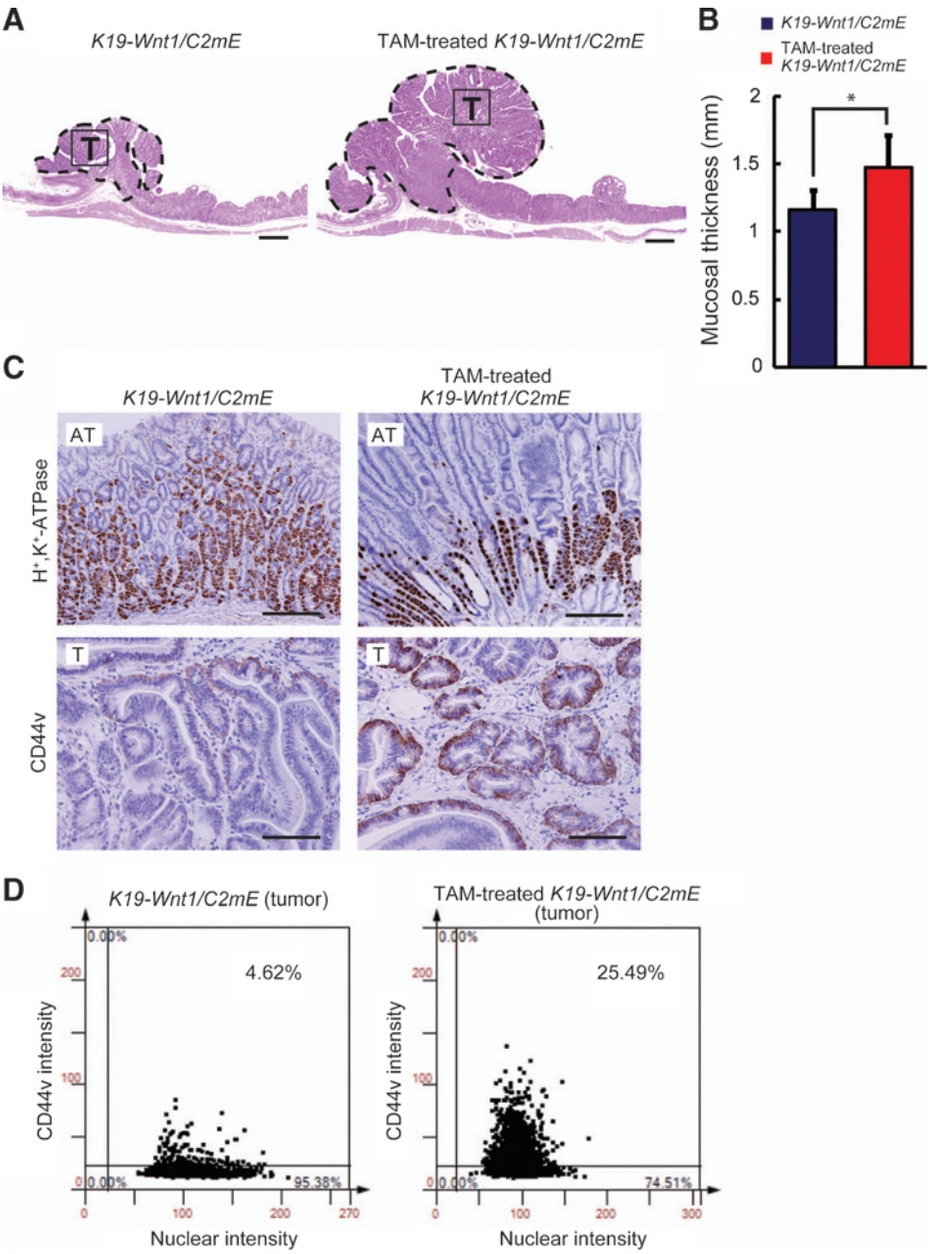

Figure 5.
Enhancement of gastric tumorigenesis by tamoxifen-induced parietal cell loss. A, hematoxylin and eosin (H&E) staining of gastric tumors (T) in 25-week-old *K19-Wnt1/C2mE* mice that had been injected with tamoxifen (or not) once a week beginning at 20 weeks of age; scale bars, 500 μm. B, mucosal thickness, which reflects the size of the tumor, in *K19-Wnt1/C2mE* mice treated (or not) with tamoxifen as determined from sections similar to those in A. Data, means ± SD for 5 mice; *, $P < 0.05$ (Student t test). C, immunohistochemical staining of H^+,K^+-ATPase and CD44v in tumor-adjacent regions (AT) and in gastric tumors (T), respectively, for 25-week-old *K19-Wnt1/C2mE* mice treated as in A; scale bars, 200 μm. D, proportion of CD44v-positive cells in gastric tumors of *K19-Wnt1/C2mE* mice treated (or not) with tamoxifen as determined from sections similar to those in C.

Tamoxifen injection promotes parietal cell loss and gastric tumor development

Given that tamoxifen treatment promoted the development of SPEM concomitant with an increase in the number of stem-like cells in WT mice, we next administered tamoxifen to *K19-Wnt1/C2mE* mice at 20 weeks of age to examine whether tamoxifen-induced parietal cell loss might also accelerate tumor development. I.p. injection of tamoxifen once a week for 5 weeks promoted the tumor growth in these mice (Fig. 5A and B). Furthermore, tamoxifen treatment enhanced the parietal cell loss as well as the production of CD44v-expressing tumor cells in *K19-Wnt1/C2mE* mice (Fig. 5C and D). Together, these results suggested that loss of parietal cells might play a role in the production of CD44v-expressing tumor cells and tumor growth in *K19-Wnt1/C2mE* mice.

Parietal cell loss is associated with increasing the number of CD44v-expressing stem-like cells

To examine the functional relevance of the *Ink4a/Arf* locus in the development of gastric tumors in *K19-Wnt1/C2mE* mice, we generated *Ink4a/Arf*$^{-/-}$ *K19-Wnt1/C2mE* mice. Tumors of *Ink4a/Arf*$^{-/-}$ *K19-Wnt1/C2mE* mice were markedly smaller than those of *K19-Wnt1/C2mE* mice (Fig. 6A and B) and were similar in size to those of *CD44*$^{-/-}$ *K19-Wnt1/C2mE* mice (16), suggesting that the *Ink4a/Arf* locus is required for CD44-dependent gastric tumor development in *K19-Wnt1/C2mE* mice. The number of parietal

Published OnlineFirst March 26, 2015; DOI: 10.1158/1940-6207.CAPR-15-0025-T

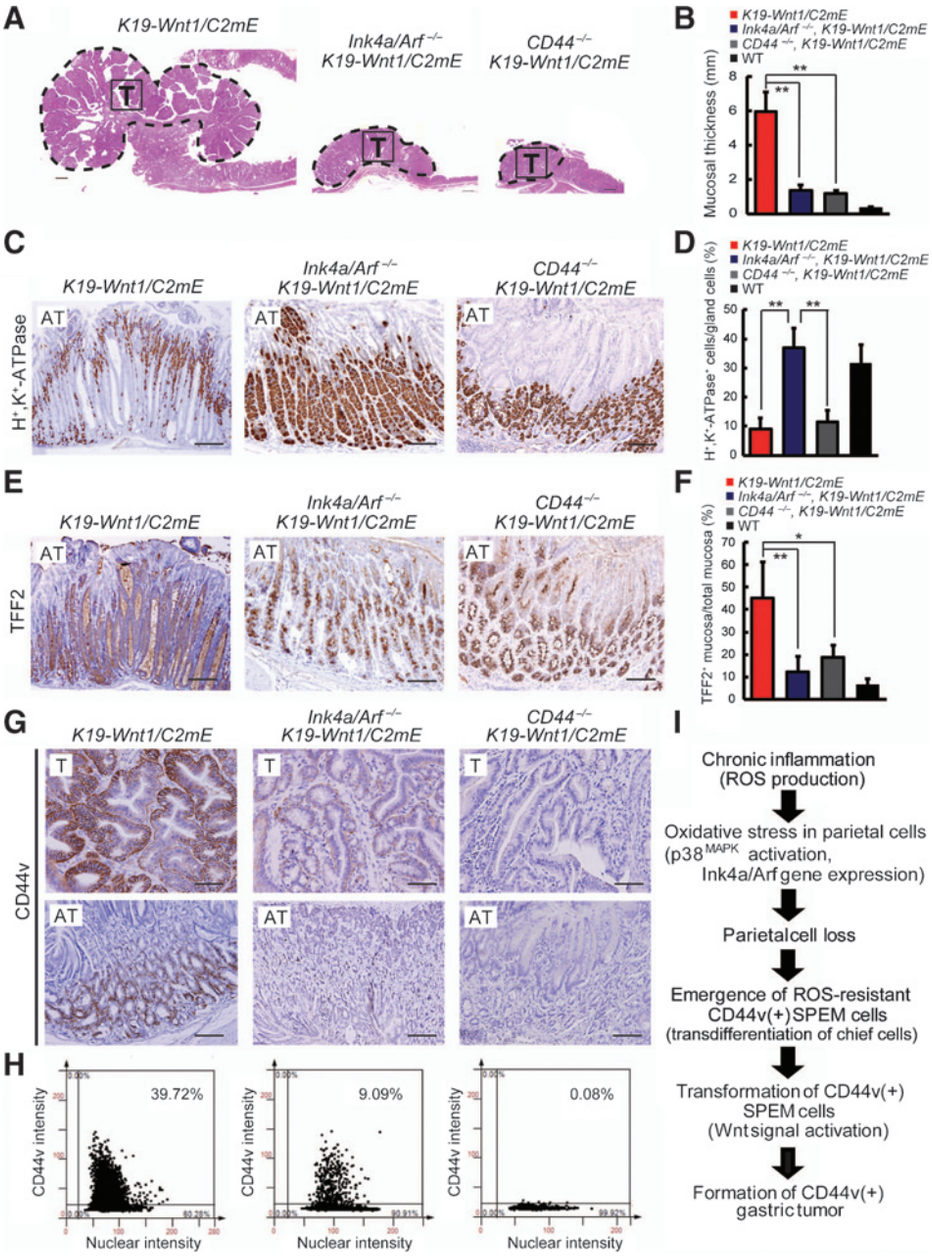

Figure 6.

The *Ink4a/Arf* locus is essential for parietal cell loss and the subsequent development of SPEM and gastric tumors. A, hematoxylin and eosin (H&E) staining of gastric tumors (T) in *K19-Wnt1/C2mE* mice, *Ink4a/Arf*$^{-/-}$ *K19-Wnt1/C2mE* mice and *CD44*$^{-/-}$ *K19-Wnt1/C2mE* mice at 30 weeks of age; scale bars, 500 μm. B, mucosal thickness, which reflects the size of the tumor, in *K19-Wnt1/C2mE* mice, *Ink4a/Arf*$^{-/-}$ *K19-Wnt1/C2mE* mice, *CD44*$^{-/-}$ *K19-Wnt1/C2mE* mice and WT mice at 30 weeks of age as determined from sections similar to those in A. Data, means ± SD for 5 mice; $^{**}P < 0.01$ (Student *t* test). C, immunohistochemical staining of H^+,K^+-ATPase in tumor-adjacent regions (AT) of 30-week-old *K19-Wnt1/C2mE* mice, *Ink4a/Arf*$^{-/-}$ *K19-Wnt1/C2mE* mice and *CD44*$^{-/-}$ *K19-Wnt1/C2mE* mice; scale bars, 200 μm. D, the mean percentage of H^+,K^+-ATPase–positive cells per gland in five microscopic fields per mouse was calculated in gastric mucosa in sections similar to those in C. Data, means ± SD for 5 mice; **, $P < 0.01$(Student *t* test). E, immunohistochemical staining of TFF2 in tumor-adjacent regions of 30-week-old *K19-Wnt1/C2mE* mice, *Ink4a/Arf*$^{-/-}$ *K19-Wnt1/C2mE* mice and *CD44*$^{-/-}$ *K19-Wnt1/C2mE* mice; scale bars, 200 μm. F, mean area of $TFF2^+$ gastric epithelium determined from sections similar to those in E. Data, means ± SD for 5 mice; *, $P < 0.05$; **, $P < 0.01$ (Student *t* test). G, immunohistochemical staining of CD44v in gastric tumors and tumor-adjacent regions in 30-week-old *K19-Wnt1/C2mE* mice, *Ink4a/Arf*$^{-/-}$ *K19-Wnt1/C2mE* mice and *CD44*$^{-/-}$ *K19-Wnt1/C2mE* mice; scale bars, 100 μm (top) or 200 μm (bottom). H, proportion of CD44v-positive cells in gastric tumors of 30-week-old *K19-Wnt1/C2mE* mice, *Ink4a/Arf*$^{-/-}$ *K19-Wnt1/C2mE* mice and *CD44*$^{-/-}$ *K19-Wnt1/C2mE* mice as determined from sections similar to those in G. I, model for metaplasia-carcinoma progression induced by chronic inflammation in the stomach. In inflamed gastric epithelium, ROS accumulate predominantly in parietal cells as a result of the low antioxidant capacity of these cells, and they activate oxidative stress–dependent signaling by $p38^{MAPK}$ that leads to the induction of *Ink4a/Arf* gene expression and consequent parietal cell loss. In response to this parietal cell loss, chief cells undergo transdifferentiation into CD44v-expressing SPEM cells that include stem-like cells with a high antioxidant capacity. Oncogenic stimulation such as activation of aberrant Wnt signaling transforms the CD44v-expressing SPEM cells into CD44v-expressing stem-like tumor cells that give rise to gastric tumors.

Published OnlineFirst March 26, 2015; DOI: 10.1158/1940-6207.CAPR-15-0025-T

cells remaining in the gastric epithelium adjacent to tumors was higher for *Ink4a/Arf*$^{-/-}$ *K19-Wnt1/C2mE* mice than for *K19-Wnt1/C2mE* mice or *CD44*$^{-/-}$ *K19-Wnt1/C2mE* mice (Fig. 6C and D), suggesting that the parietal cell loss in the initial stage of gastric tumorigenesis is regulated by the *Ink4a/Arf* locus but not by CD44 expression. On the other hand, the development of SPEM was significantly suppressed in both *Ink4a/Arf*$^{-/-}$ *K19-Wnt1/C2mE* mice and *CD44*$^{-/-}$ *K19-Wnt1/C2mE* mice compared with *K19-Wnt1/C2mE* mice (Fig. 6E and F), suggesting that the suppression of SPEM development in *Ink4a/Arf*$^{-/-}$ *K19-Wnt1/C2mE* mice and *CD44*$^{-/-}$*K19-Wnt1/C2mE* mice is mediated by different mechanisms. The *Ink4a/Arf* locus is essential for the parietal cell loss, whereas CD44 is required for the expansion of SPEM after parietal cell loss.

Our results indicated that the stem-like cells in SPEM might be the cells of origin for CD44v-expressing tumor cells in *K19-Wnt1/C2mE* mice; therefore, we examined whether the suppression of CD44v-expressing SPEM development might reduce the production of CD44v-expressing tumor cells in *Ink4a/Arf*$^{-/-}$ *K19-Wnt1/C2mE* mice. The area of CD44v-expressing tumor cells was found to be greatly reduced in *Ink4a/Arf*$^{-/-}$ *K19-Wnt1/C2mE* mice compared with *K19-Wnt1/C2mE* mice (Fig. 6G and H). Given that SPEM is a precancerous lesion of gastric cancer, these results suggest that CD44v-expressing metaplastic cells produced as a result of parietal cell loss might subsequently undergo conversion to CD44v-expressing tumor cells in *K19-Wnt1/C2mE* mice (Fig. 6I).

Discussion

Gastrointestinal malignancies are strongly linked to chronic inflammation (25–29). Gastric tumorigenesis in *K19-Wnt1/C2mE* mice was also recently shown to be suppressed by knockout of either TNFα or its receptor TNFR1, suggesting that TNFα-dependent inflammation plays a key role in the development of gastric cancer (30). Furthermore, the development of SPEM in response to acute parietal cell loss is dependent on the recruitment of macrophages to the gastric epithelium (31). Together, these findings suggest that inflammation triggers the histopathologic alterations of gastric epithelium that leads to tumor development. We have now shown that the inflammation-associated ROS plays a key role in the parietal cell loss that is an early and critical step in the development of SPEM, and the subsequent formation of gastric tumors. The accumulation of ROS triggers the $p38^{MAPK}$–$p16^{INK4a}$/$p19^{ARF}$ signaling pathway selectively in parietal cells and the consequent induction of parietal cell loss. In fact, parietal cells have been reported to contain abundant mitochondria (32), a major source of intrinsic ROS production, and have been considered to be highly susceptible to oxidative stress (33). Together, oxidative stress–dependent $p38^{MAPK}$–$p16^{INK4a}$/$p19^{ARF}$ signaling is activated selectively in parietal cells of the stomach epithelium in the presence of high ROS level.

The *Ink4a/Arf* locus encodes the cyclin-dependent kinase inhibitor $p16^{INK4a}$ as well as $p19^{ARF}$, both of which have been shown to induce cell-cycle arrest, senescence, and apoptosis in response to oncogenic stimulation (34, 35). These proteins are thought to serve as key regulators in tumor-suppressor networks that are often disabled in human cancers (35). However, our present results indicate that ROS-induced expression of $p16^{INK4a}$ and $p19^{ARF}$ promotes gastric tumorigenesis by inducing parietal cell loss and the emergence of CD44v-expressing SPEM cells. The activation of tumor-suppressor networks might, thus, promote carcinogenesis in some cases through induction of the loss of gatekeeper cells that play an important role in epithelial homeostasis.

Carcinogenesis is often coupled to the generation of ROS, and cancer cells have, therefore, evolved mechanisms to protect themselves from oxidative stress through upregulation of both antioxidants and prosurvival molecules (36, 37). Expression of CD44v promotes cystine transport via system xc(−), and thereby contributes to ROS defense by increasing the synthesis of reduced glutathione in cancer cells (16). We previously showed that the *de novo* expression of CD44v in metaplasia cells potentiates ROS defense in these cells, and thereby promotes the development of SPEM (17). Depletion of CD44 or treatment with the xCT inhibitor sulfasalazine markedly suppressed the development of SPEM and gastric tumors in *K19-Wnt1/C2mE* mice (16, 17), and the expression of SPEM-related genes was found to be greatly increased in CD44v-expressing tumor cells compared with CD44-negative tumor cells in this model (17). We have now found that, compared with normal gastric mucosa, SPEM induced as a result of *Ink4a/Arf*–dependent parietal cell loss contains an increased number of CD44v-expressing stem-like cells that are capable of initiating gastric organoid formation. Gastric organoids established from SPEM were found to express high level of *Troy* mRNA (data not shown), suggesting that *Troy*-expressing chief cells, which act as the reserve stem cells in response to gastric tissue damage, might be the candidate source of CD44v-expressing stem-like cells. Our results thus suggest that, in gastric tumorigenesis, it is likely that CD44v-expressing stem-like cells in SPEM undergo conversion to CD44v-expressing tumor cells, possibly as a result of the activation of oncogenic Wnt signaling or other genetic or epigenetic events (Fig. 6I).

In conclusion, our present data provide evidence that ROS promote gastric tumorigenesis through the induction of $p38^{MAPK}$–$p16^{INK4a}$/$p19^{ARF}$ signaling in parietal cells—cells that serve as gatekeepers for homeostasis in oxyntic glands.

Disclosure of Potential Conflicts of Interest

No potential conflicts of interest were disclosed.

Authors' Contributions

Conception and design: R. Seishima, J.R. Goldenring, H. Saya, O. Nagano
Development of methodology: T. Wada, K. Tsuchihashi
Acquisition of data (provided animals, acquired and managed patients, provided facilities, etc.): R. Seishima, T. Wada, M. Yoshikawa
Analysis and interpretation of data (e.g., statistical analysis, biostatistics, computational analysis): R. Seishima, T. Wada, K. Tsuchihashi, M. Yoshikawa, H. Hasegawa
Writing, review, and/or revision of the manuscript: R. Seishima, J.R. Goldenring, O. Nagano
Administrative, technical, or material support (i.e., reporting or organizing data, constructing databases): S. Okazaki, H. Oshima, M. Oshima, T. Sato
Study supervision: H. Hasegawa, Y. Kitagawa, O. Nagano

Acknowledgments

The authors thank I. Ishimatsu, Y. Suzuki, and S. Hayashi for technical assistance as well as M. Sato for help in preparation of the article.

Grant Support

This work was supported by grants (to H. Saya) from, as well as in part by the Project for Development of Innovative Research on Cancer Therapeutics

(P-Direct; to O. Nagano) of, the Ministry of Education, Culture, Sports, Science, and Technology of Japan. Department of Veterans Affairs Merit Review award and NIH RO1 DK071590 (to J.R. Goldenring).

The costs of publication of this article were defrayed in part by the payment of page charges. This article must therefore be hereby marked *advertisement* in accordance with 18 U.S.C. Section 1734 solely to indicate this fact.

Received January 22, 2015; revised March 16, 2015; accepted March 22, 2015; published OnlineFirst March 26, 2015.

References

1. Genta RM. Helicobacter pylori, inflammation, mucosal damage, and apoptosis: pathogenesis and definition of gastric atrophy. Gastroenterology 1997;113:S51–5.
2. Dixon MF. Prospects for intervention in gastric carcinogenesis: reversibility of gastric atrophy and intestinal metaplasia. Gut 2001;49:2–4.
3. Nam KT, Lee HJ, Sousa JF, Weis VG, O'Neal RL, Finke PE, et al. Mature chief cells are cryptic progenitors for metaplasia in the stomach. Gastroenterology 2010;139:2028–37 e9.
4. Goldenring JR, Nam KT, Mills JC. The origin of pre-neoplastic metaplasia in the stomach: chief cells emerge from the Mist. Exp Cell Res 2011;317:2759–64.
5. Schmidt PH, Lee JR, Joshi V, Playford RJ, Poulsom R, Wright NA, et al. Identification of a metaplastic cell lineage associated with human gastric adenocarcinoma. Lab Invest 1999;79:639–46.
6. Nozaki K, Ogawa M, Williams JA, Lafleur BJ, Ng V, Drapkin RI, et al. A molecular signature of gastric metaplasia arising in response to acute parietal cell loss. Gastroenterology 2008;134:511–22.
7. Federico A, Morgillo F, Tuccillo C, Ciardiello F, Loguercio C. Chronic inflammation and oxidative stress in human carcinogenesis. Int J Cancer 2007;121:2381–6.
8. Waris G, Ahsan H. Reactive oxygen species: role in the development of cancer and various chronic conditions. J Carcinog 2006;5:14.
9. Xia Z, Dickens M, Raingeaud J, Davis RJ, Greenberg ME. Opposing effects of ERK and JNK-p38 MAP kinases on apoptosis. Science 1995;270:1326–31.
10. Wu WS. The signaling mechanism of ROS in tumor progression. Cancer Metastasis Rev 2006;25:695–705.
11. Macleod KF. The role of the RB tumour suppressor pathway in oxidative stress responses in the haematopoietic system. Nat Rev Cancer 2008;8:769–81.
12. Aruffo A, Stamenkovic I, Melnick M, Underhill CB, Seed B. CD44 is the principal cell surface receptor for hyaluronate. Cell 1990;61:1303–13.
13. Ponta H, Sherman L, Herrlich PA. CD44: from adhesion molecules to signalling regulators. Nat Rev Mol Cell Biol 2003;4:33–45.
14. Nagano O, Saya H. Mechanism and biological significance of CD44 cleavage. Cancer Sci 2004;95:930–5.
15. Tanabe KK, Ellis LM, Saya H. Expression of CD44R1 adhesion molecule in colon carcinomas and metastases. Lancet 1993;341:725–6.
16. Ishimoto T, Nagano O, Yae T, Tamada M, Motohara T, Oshima H, et al. CD44 variant regulates redox status in cancer cells by stabilizing the xCT subunit of system xc(-) and thereby promotes tumor growth. Cancer Cell 2011;19:387–400.
17. Wada T, Ishimoto T, Seishima R, Tsuchihashi K, Yoshikawa M, Oshima H, et al. Functional role of CD44v-xCT system in the development of spasmolytic polypeptide-expressing metaplasia. Cancer Sci 2013;104:1323–9.
18. Mayer B, Jauch KW, Gunthert U, Figdor CG, Schildberg FW, Funke I, et al. *De novo* expression of CD44 and survival in gastric cancer. Lancet 1993;342:1019–22.
19. Lau WM, Teng E, Chong HS, Lopez KA, Tay AY, Salto-Tellez M, et al. CD44v8–10 is a cancer-specific marker for gastric cancer stem cells. Cancer Res 2014;74:2630–41.
20. Oshima H, Matsunaga A, Fujimura T, Tsukamoto T, Taketo MM, Oshima M. Carcinogenesis in mouse stomach by simultaneous activation of the Wnt signaling and prostaglandin E_2 pathway. Gastroenterology 2006;131:1086–95.
21. Sugihara E, Shimizu T, Kojima K, Onishi N, Kai K, Ishizawa J, et al. Ink4a and Arf are crucial factors in the determination of the cell of origin and the therapeutic sensitivity of Myc-induced mouse lymphoid tumor. Oncogene 2012;31:2849–61.
22. Bjerknes M, Cheng H. Multipotential stem cells in adult mouse gastric epithelium. Am J Physiol Gastrointest Liver Physiol 2002;283:G767–777.
23. Huh WJ, Khurana SS, Geahlen JH, Kohli K, Waller RA, Mills JC. Tamoxifen induces rapid, reversible atrophy, and metaplasia in mouse stomach. Gastroenterology 2012;142:21–4 e7.
24. Barker N, Huch M, Kujala P, vande Wetering M, Snippert HJ, van Es JH, et al. Lgr5(+ve) stem cells drive self-renewal in the stomach and build long-lived gastric units *in vitro*. Cell Stem Cell 2010;6:25–36.
25. Ullman TA, Itzkowitz SH. Intestinal inflammation and cancer. Gastroenterology 2011;140:1807–16.
26. Shacter E, Weitzman SA. Chronic inflammation and cancer. Oncology 2002;16:217–26, 29; discussion 30–2.
27. Coussens LM, Werb Z. Inflammation and cancer. Nature 2002;420:860–7.
28. Itzkowitz SH, Yio X. Inflammation and cancer IV. Colorectal cancer in inflammatory bowel disease: the role of inflammation. Am J Physiol Gastrointest Liver Physiol 2004;287:G7–17.
29. Ernst PB, Gold BD. The disease spectrum of Helicobacter pylori: the immunopathogenesis of gastroduodenal ulcer and gastric cancer. Annu Rev Microbiol 2000;54:615–40.
30. Oshima H, Ishikawa T, Yoshida GJ, Naoi K, Maeda Y, Naka K, et al. TNF-alpha/TNFR1 signaling promotes gastric tumorigenesis through induction of Noxo1 and Gna14 in tumor cells. Oncogene 2014;33:3820–9.
31. Peterson CP, Weis VG, Nam KT, Sousa JF, Fingleton B, Goldenring JR. Macrophages promote progression of spasmolytic polypeptide expressing metaplasia after acute loss of parietal cells. Gastroenterology 2014;146:1727–38 e8.
32. Sannes PL, Katsuyama T, Spicer SS. Chemical properties of mitochondria in the gastric parietal cell. J Histochem Cytochem 1979;27:873–7.
33. Jones MK, Zhu E, Sarino EV, Padilla OR, Takahashi T, Shimizu T, et al. Loss of parietal cell superoxide dismutase leads to gastric oxidative stress and increase injury susceptibility in mice. Am J Physiol Gastrointest Liver Physiol 2011;301:G537–46.
34. Takahashi A, Ohtani N, Yamakoshi K, Iida S, Tahara H, Nakayama K, et al. Mitogenic signalling and the p16INK4a-Rb pathway cooperate to enforce irreversible cellular senescence. Nat Cell Biol 2006;8:1291–7.
35. Sharpless NE. INK4a/ARF: a multifunctional tumor suppressor locus. Mutat Res 2005;576:22–38.
36. Nogueira V, Hay N. Molecular pathways: reactive oxygen species homeostasis in cancer cells and implications for cancer therapy. Clin Cancer Res 2013;19:4309–14.
37. Nagano O, Okazaki S, Saya H. Redox regulation in stem-like cancer cells by CD44 variant isoforms. Oncogene 2013;32:5191–8.

Published OnlineFirst March 26, 2015; DOI: 10.1158/1940-6207.CAPR-15-0025-T

Cancer Prevention Research

Ink4a/Arf-Dependent Loss of Parietal Cells Induced by Oxidative Stress Promotes CD44-Dependent Gastric Tumorigenesis

Ryo Seishima, Takeyuki Wada, Kenji Tsuchihashi, et al.

Cancer Prev Res 2015;8:492-501. Published OnlineFirst March 26, 2015.